Prediction of the lowest-energy structures of rare-earth metallic clusters with a Möbius inversion pair potential

You-Hua Luo[1,2] and Yuzhu Wang[1,*]
[1]*Laboratory for Quantum Optics, Shanghai Institute of Optics and Fine Mechanics, Chinese Academy of Sciences, P.O. Box 800-211, Shanghai 201800, China*
[2]*Department of Physics, Henan University, Kaifeng 475001, China*
(Received 20 December 2000; published 30 May 2001)

The Möbius inversion pair potential has been employed, in combination with genetic algorithms, to predict the lowest-energy structures of the rare-earth metallic clusters La_N, Ce_N, and Pr_N ($N=3-20$). Results are given for the symmetries, binding energies, nearest-neighbor distances of these clusters, and lowest-energy configurations of Ce_N clusters. Also, the calculated second finite difference of the total energy shows that for three species elements, the 13-atom clusters with I_d symmetry are particularly stable. Some minor peaks are also found at size $N=4$, 6, 11, and 15, which indicates that the corresponding clusters are relatively stable in structure. Present work points out a route to studying clusters.

DOI: 10.1103/PhysRevA.64.015201 PACS number(s): 36.40.Mr, 36.40.Qv, 61.46.+w

Introduction. The history of studying clusters can be traced back to the work by Becker in 1956, in which he reported the experimental method of producing cluster beams [1]. However, the great advancement of cluster physics had not been achieved until in 1983. Both the discovery of the magic number structure of the alkali metal clusters in 1984 [2] and the finding of the C_{60} cluster in 1985 [3] are two milestones. They impel directly the progress of cluster investigations. The magic number of a cluster indicates that the cluster with certain size is more stable in structure than neighboring clusters. The C_{60} cluster, especially stable, and its solid [4], demonstrate sufficiently that the cluster with high stability can be found in nature. The motivation to study the lowest-energy structure of a cluster is first to find the cluster with high stability, and second to understand its evolution from individual atom to bulk. So far, an enormous effort has been devoted to determining the lowest-energy structures of alkali metal clusters, inert gaseous clusters, transition-metal clusters, and semiconductor clusters. The methods used to determine the lowest-energy structure of a cluster are almost empirical or semiempirical ones. The first principles or *ab initio* calculations are very difficult for a cluster with more than ten atoms, due to the high dimensionality of the energy hypersurfaces governing the structure of the systems that gives rise to many local minima. On the other hand, the potential to describe the interaction between atoms constitutes the key ingredient in determining the lowest-energy structure of a cluster. Nevertheless, it is also quite difficult to obtain a reliable interatomic interaction potential. At present, some empirical or semiempirical potentials, such as Lennard-Jones potential, embedded-atom model, and tight-binding Gupta-type potential, etc., are often employed. There are some adjusting parameters in the formalism of these potentials; their reliability could not be guaranteed in predicting the lowest-energy structure of a cluster.

In this paper, we employ the Möbius inversion pair potential, which is directly derived from the cohesive energy of bulk materials, in conjunction with genetic algorithms, to predict the lowest-energy structures of the rare-earth metallic clusters La_N, Ce_N, and Pr_N ($N=3-20$). To our knowledge, the lowest-energy structures of the rare-earth metallic clusters have not been reported up to now. In the following, we will describe the details of the Möbius inversion pair potential and briefly introduce genetic algorithms.

Möbius inversion pair potential and genetic algorithms. In 1990, the Möbius inversion theorem, an old one in number theory, was applied to solve skillfully a few inversion problems in physics by Chen [5]. That effort was highly appraised [6]. Based on this theorem, the Möbius transform formulas for sc, fcc, bcc, hcp, and dhcp structures have been obtained [7–10]. The interatomic interaction potential can be derived from the cohesive energy of bulk materials by using the Möbius transform formulas. In general, the cohesive energy per atom in a crystal structure can be expressed as [11]

$$E(r)=\frac{(1/N)}{2!}\sum_{i\neq j}\Phi^2(r_{ij})+\frac{(1/N)}{3!}\sum_{i\neq j\neq k}\Phi^3(r_{ij},r_{jk},r_{ki})+\ldots, \tag{1}$$

where r is the lattice constants, Φ^2 and Φ^3 are the two-body and three-body interatomic potentials, respectively, and r_{ij} represents the displacement vector from the ith atom to the jth atom. In first-order approximation, the multibody interactions can be ignored. For the rare-earth metals with a dhcp structure, the binding energy per atom can be simplified as (for details, see Ref. [10])

$$E(r)=\sum_{i=1}^{7}E_i. \tag{2}$$

By introducing an operator G, $Gf(r)=3\Sigma_{n=1}^{\infty}f(nr)+6\Sigma_{n=1}^{\infty}f(\sqrt{3+\alpha^2/4}nr)$, which comes from the terms satisfying $m=n=1$ in $E_1(r)$ and $E_5(r)$, the cohesive energy can be rewritten as $E(r)=G\Phi(r)+R\Phi(r)$, where the operator R is defined as

$$R\Phi(r)=6\sum_{m,n,l=1}^{\infty}{}'\,\Phi(\sqrt{(m^2+n^2+mn)+(l\alpha/2)^2}r)+E_2(r)+E_3(r)+E_4(r)+E_6(r)+E_7(r).$$

*Author to whom the correspondence should be addressed.

TABLE I. Values of u_0 (in eV), r_0 (in Å), and β (in Å^{-1}) in the Möbius inversion pair potential.

Atoms	u_0	r_0	β
La	0.6654	3.2250	0.6335
Ce	0.6207	3.2134	0.6207
Pr	0.5377	3.2200	0.6301

The symbol Σ' means that the terms with $m=n=1$ are not included. In order to obtain the pair potential between the rare-earth metallic atoms from the cohesive energy, the other operator N need to be introduced, namely, $Nf(r) = \frac{1}{3}\sum_{n,l=1}^{\infty}\mu(l)(-2)^{n-1}f[(3+\alpha^2/4)^{(n-1)/2}lr]$, where $\mu(l)$ is the Möbius function [5]. According to the Möbius inversion theorem and introduced above two operators N and R, the interatomic interaction potential for the rare-earth metals can be written as

$$\Phi(r)=(N-NRN+NRNRN-,\ldots,)E(r). \tag{3}$$

For simplicity, the atomic pair potential of the rare earth metals can be fitted by the following Morse-type analytic expression [10]:

$$\Phi(r)=u_0\{\exp[-2\beta(r-r_0)]-2\ \exp[-\beta(r-r_0)]\}, \tag{4}$$

where r denotes interatomic distance, and u_0, r_0, and β are parameters fitted, their values are listed in Table I. In what follows, we argue that the Möbius inversion pair potential is reliable in determining the lowest-energy structure of a small metallic cluster. For the rare-earth metallic clusters, in the absence of *ab initio* results and that obtained by other methods, a direct comparison is not possible. Thus, our results for fully optimized cluster geometries of the rare-earth metallic atoms with $3\leqslant n\leqslant 20$ may be considered as predictions. Here, by using the Möbius inversion pair potential of Ni as a function of distance between atoms [11],

$$\phi(r)=0.4031\{\exp[-2.6632(r-2.852)] - 2\ \exp[-1.3316(r-2.852)]\},$$

we present our results for small nickel clusters, for which some *ab initio* results [12] and tight-binding molecular-dynamics (TBMD) calculations [13] are available for comparison. In Table II, the symmetry, binding energy per atom, and average bond lengths are given for Ni_n ($n=3$–7) clusters. It is found that our results are in good agreement with *ab initio* calculations [12], especially the binding energy per atom. Of course, we also noted that there are some discrepancies between results calculated by the Möbius inversion pair potential and those obtained by *ab initio* methods. The main reason is that the majority of the existing *ab initio* data for Ni clusters with $n\geqslant 3$, even when optimization is carried out, refer only to symmetry-restricted geometries [13]. For example, for $n=3$, Basch *et al.* [12] reported a detailed optimization study only for one type of cluster symmetry, $D_{\infty h}$. However, from the fact that results obtained by the Möbius inversion pair potential, which is a simple two-body form, can compare with those given by *ab initio* calculations, we confirm that the Möbius inversion pair potential directly derived from the cohesive energy of bulk materials by means of the Möbius inversion theorem, can be used to study small metallic clusters. Such interatomic potentials are credible in determining the lowest-energy structures of metallic atomic clusters.

In this paper, the genetic algorithms (GA) is used to optimize the geometric configuration of a cluster. The GA has become a powerful method to search for the most stable structure of a cluster [14]. The practical operation of GA used here is basically the same as that performed in our previous work [15]. In general, it can be divided into three essential steps: selection, crossover, and mutation. For a given cluster size, we first generate a population containing of p ($p=16$ in present) distinct individuals at random. Then two individuals in the population are selected as ''parent'' to generate a new ''child.'' The possibility of being chosen as parent is set to be identical for all the candidates in population. By setting the ''mating'' and ''mutation'' rate appropriately, the GA can carry out an exhaustive search on the potential energy surface within acceptable steps. After a child is produced, it is optimized by the conjugate-gradient minimization routine, which is used to relax the cluster to a reasonable local minimum nearby. In our simulation, iteration steps are set 1000 to 5000 in order to make sure that both the lowest-energy structure of a cluster is invariant

TABLE II. Binding energies (in eV/atom) and average bond lengths (in Å) for Ni_n ($n=3$–7) clusters with Möbius inversion pair potential, and compared with previous *ab initio* results[a] and TBMD calculations.[b]

Cluster	Symmetry			Binding energy			Average bond lengths		
	ab initio	TBMD	present	*ab initio*	TBMD	present	*ab initio*	TBMD	present
Ni_3	$D_{\infty h}$			0.50			2.38		
Ni_3	D_{3h}	D_{3h}	D_{3h}	0.45	1.66	0.40	2.49	2.30	2.85
Ni_4	$D_{\infty h}$			0.58			2.49		
Ni_4	D_{4h}	D_{4h}		0.58	1.87		2.49	2.26	
Ni_4	T_d		T_d	0.32		0.61	2.49		2.85
Ni_5	C_{4v}	T_d	D_{3h}	0.71	2.16	0.74	2.49	2.42	2.84
Ni_6	O_h	D_{4h}	O_h	0.72	2.36	0.88	2.49	2.47	2.81
Ni_7		D_{5h}	D_{5h}		2.42	0.97	2.51	2.82	

[a]Reference [12]. [b]Reference [13].

TABLE III. Calculated results for the lowest-energy structures of the rare-earth metallic clusters up to size $N=20$, including symmetry, binding energy (in eV), and nearest-neighbor distance (in Å).

	Symmetry			Binding energy			Nearest-neighbor distance		
N	La_N	Ce_N	Pr_N	La_N	Ce_N	Pr_N	La_N	Ce_N	Pr_N
3	D_{3h}	D_{3h}	D_{3h}	0.665	0.621	0.538	3.225	3.213	3.220
4	T_d	T_d	T_d	0.998	0.931	0.807	3.225	3.213	3.220
5	D_{3h}	D_{3h}	D_{3h}	1.268	1.185	1.025	3.088	3.071	3.081
6	O_h	O_h	O_h	1.565	1.463	1.265	3.101	3.087	3.096
7	D_{5h}	D_{5h}	D_{5h}	1.783	1.670	1.443	2.890	2.867	2.882
8	D_{2d}	D_{2d}	D_{2d}	2.011	1.886	1.627	2.844	2.818	2.835
9	D_{3h}	D_{3h}	D_{3h}	2.228	2.092	1.804	2.869	2.844	2.860
10	D_{3h}	D_{3h}	D_{3h}	2.433	2.287	1.971	2.645	2.625	2.638
11	D_{4d}	D_{4d}	D_{4d}	2.660	2.502	2.155	2.675	2.656	2.668
12	C_{2v}	C_{2v}	C_{2v}	2.859	2.692	2.317	2.571	2.694	2.708
13	I_d	I_d	I_d	3.097	2.915	2.509	2.759	2.736	2.752
14	C_2	C_2	C_2	3.250	3.064	2.634	2.533	2.507	2.525
15	D_{6d}	D_{6d}	D_{6d}	3.430	3.237	2.781	2.579	2.552	2.570
16	D_{3h}	D_{3h}	D_{3h}	3.591	3.393	2.913	2.446	2.417	2.436
17	D_{3h}	D_{3h}	D_{3h}	3.750	3.546	3.042	1.989	1.956	1.978
18	C_{2v}	C_{2v}	C_{2v}	3.918	3.708	3.179	1.943	1.911	1.933
19	D_{5h}	D_{5h}	D_{5h}	4.084	3.868	3.315	1.986	1.946	1.973
20	C_1	C_1	C_1	4.236	4.016	3.439	1.954	1.896	1.940

within 1000 mating operations and the global minima of La_N, Ce_N, and Pr_N clusters up to $N=20$ can be obtained.

Results and discussion. We have predicted the lowest-energy structures of the rare-earth metallic clusters La_N, Ce_N, and Pr_N up to 20 atoms by using the Möbius inversion pair potential and genetic algorithms. The symmetry, binding energy and nearest-neighbor distance of these clusters are summarized in Table III. The results show that at the same size, La_N, Ce_N, and Pr_N clusters have the same point group. For La_{13}, Ce_{13}, and Pr_{13}, their symmetry is highest; while La_{20}, Ce_{20}, and Ce_{20}, their symmetry is lowest, being disordered. In order to visually understand the symmetrical characteristic of these clusters, in Fig. 1 we have plotted the lowest-energy configurations of Ce_N clusters up to $N=20$. For cerium trimer, equilateral triangle geometry with D_{3h} symmetry is lower in energy than an isosceles triangle. In the case of Ce_4, the tetrahedron with T_d group is lower in energy than planar rhombus geometry, which is different from noble metal clusters [16]. The lowest-energy structure found for Ce_5 is a trigonal bipyramid with D_{3h} symmetry. For Ce_6, the octahedron geometry with O_h symmetry is found to the lowest-energy structure. For Ce_7, its lowest-energy structure is the pentagonal bipyramid geometry with D_{5h} symmetry. The lowest-energy strucuture of Ce_8 can be regarded as a distorted bicapped octahedron, and the octahedron is capped on adjacent faces. We found that the D_{3h} tricapped trigonal prism is the minimum energy structure of Ce_9. In what follows, we give an explanation for the atomic structures of a few clusters with high symmetry, such as Ce_{13}, Ce_{15}, and Ce_{19}. The lowest-energy structure of Ce_{13} is an icosahedron with I_d symmetry. This geometry has also been found in the 13-atom cluster of most elements. In fact, the pentagonal bipyramid geometry of Ce_7 is also common for the 7-atom cluster of many species. The minimum energy geometries of Ce_{15} and Ce_{19} are the tetrahexahedron and double-icosahedron, respectively. The double-icosahedron geometry was found in the 19-atom cluster of inert gases and transition-metal rhodium, but the tetrahexahedron one was found only in the 15-atom cluster of transition-metal rhodium [17].

The higher the symmetry, is the cluster more stable? In Fig. 2 for the La_N, Ce_N, and Pr_N clusters we have displayed the calculated second finite difference of the total minimum energy, $\Delta_2 E(N)=E(N+1)+E(N-1)-2E(N)$, as a function of cluster size. A peak in $\Delta_2 E(N)$ indicates that the cluster of size N is more stable than neighboring clusters. The results show that the prominent $\Delta_2 E(N)$ peaks occur at $N=13$. It means that the 13-atom clusters of La, Ce, and Pr elements are particularly stable, i.e., the size 13 is a ''magic number.'' A few secondary peaks are also found at size $N=4$, 6, 11, and 15. It demonstrates that the corresponding clusters are relative stable. It is noted that the symmetry of the 7-atom cluster is higher than that of the cluster at size $N=11$. However, the 7-atom cluster is not stable in structure. It illustrates that the cluster with high symmetry is not always more stable than that with low symmetry. It is easily understood by Jahn-Teller effects.

Finally, it is necessary to point out that the Möbius inversion pair potential employed here is only a first-order approximation. For the medium-sized clusters, the three-body interaction should be taken into account. From the calculated average binding energies and nearest-neighbor distances of three rare-earth metallic clusters, as listed in Table III, we noted that the average cohesive energies increase with in-

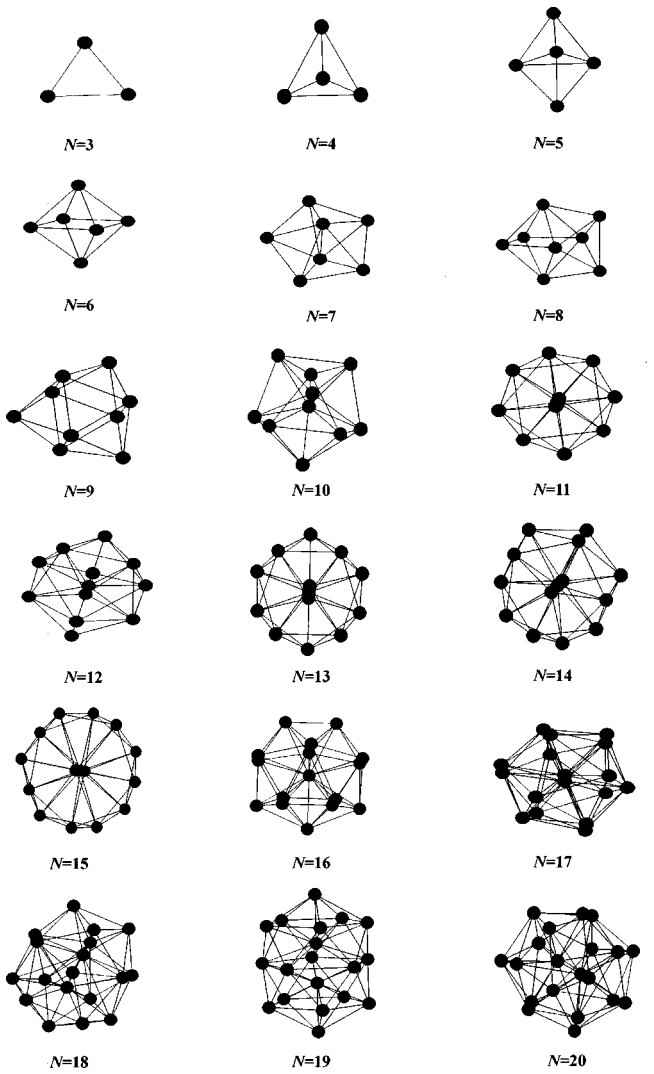

FIG. 1. Lowest-energy configurations of Ce_N clusters up to 20 atoms, calculated by Möbius inversion pair potential.

creasing cluster size, and the nearest-neighbor distances fluctuate with increasing cluster size. These characteristics are reasonable, but for the clusters with size $N \geqslant 17$, the nearest-neighbor distances are too small. Therefore, we conjecture

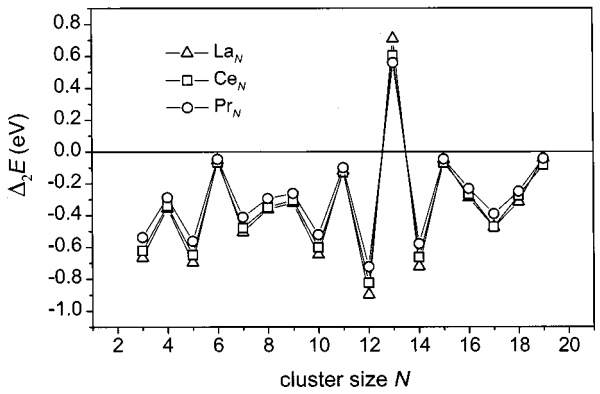

FIG. 2. Calculated second finite differences of the total energies of the rare-earth metallic clusters, La_N (triangles), Ce_N (squares), and Pr_N (circles). Lines joining points are merely visual aids.

that the effect of the three-body interaction on the lowest-energy structures of the rare-earth metallic clusters with size $N \geqslant 17$ might be significant.

In summary, in the present paper we have employed the Möbius inversion pair potential and genetic algorithms, to predict the lowest-energy structures of the rare-earth metallic clusters up to 20 atoms. We have calculated the symmetries, binding energies, nearest-neighbor distances of La_N, Ce_N, and Pr_N clusters, and lowest-energy configurations of Ce_N clusters. The second finite difference of the total energy is also calculated. Our results indicate that at size $N=4$, 6, 11, 13, and 15, the clusters are more stable than neighboring ones, especially the 13-atom cluster. In addition, from the above discussion we can come to the conclusion that the cluster with high symmetry is not always more stable than that with low symmetry. It can be explained by means of Jahn-Teller effects. Also, the effect of the three-body interaction on the lowest-energy structures of the rare-earth metallic clusters with the medium-size should be considered.

Acknowledgments. This work was supported by National Natural Science Foundation of China Grant No. 19834060, and Ministry of Science and Technique of China Grant No. 95-Yu-34. Y.H. Luo is also grateful to the Natural Science Foundation of Henan Province for their financial support.

[1] E. W. Becker, Z. Phys. **146**, 333 (1956).
[2] W. D. Knight, K. Clemenger, W. A. de Heer, W. A. Saunders, M. Y. Chou, and M. L. Cohen, Phys. Rev. Lett. **52**, 2141 (1984).
[3] H. W. Kroto, J. R. Heath, S. C. O'Brian, R. F. Curl, and R. E. Smalley, Nature (London) **318**, 162 (1985).
[4] W. Krätschemer, L. D. Lamb, K. Fostiropoulos, and D. R. Huffman, Nature (London) **347**, 354 (1990).
[5] N. X. Chen, Phys. Rev. Lett. **64**, 1193 (1990).
[6] J. Maddox, Nature (London) **344**, 377 (1990).
[7] N. X. Chen, Y. Chen, and G. Y. Li, Phys. Lett. A **149**, 357 (1990).
[8] N. X. Chen and G. B. Ren, Phys. Lett. A **160**, 319 (1991).
[9] N. X. Chen and G. B. Ren, Phys. Rev. B **45**, 8177 (1992).
[10] S. Q. Yang, W. X. Zhang, J. Gong, W. L. Zhang, and H. C. Wang, Acta Phys. Sin. (Overseas Ed.) **8**, 801 (1999).
[11] S. J. Liu, M. Li, and N. X. Chen, J. Phys.: Condens. Matter **5**, 4381 (1993).
[12] H. Basch, M. D. Newton, and J. W. Moskowitz, J. Chem. Phys. **73**, 4492 (1980).
[13] M. Menon, J. Connolly, N. Lathiotakis, and A. Andriotis, Phys. Rev. B **50**, 8903 (1994).
[14] D. M. Deaven and K. M. Ho, Phys. Rev. Lett. **75**, 288 (1995). See also, J. Maddox, Nature (London) **376**, 209 (1995).
[15] Y. H. Luo, S. Q. Qiu, J. J. Zhao, and G. H. Wang, Phys. Rev. B **59**, 14 903 (1999).
[16] J. J. Zhao, Y. H. Luo, and G. H. Wang, Euro. Phys. J. D (to be published).
[17] H. Q. Sun, Y. Ren, Y. H. Luo, and G. H. Wang, Physica B **293**, 260 (2001).